Dynamics of $^1S_0$ diproton formation in the $pd \to \{pp\}_s n$ and $pN \to \{pp\}_s \pi$ reactions in the GeV region

Yu.N. Uzikov[1], J. Haidenbauer[2], C. Wilkin[3]
[1] *Laboratory of Nuclear Problems, Joint Institute for Nuclear Research, 141980 Dubna, Russia*
[2] *Institut für Kernphysik (Theorie), Forschungszentrum Jülich, 52425 Jülich, Germany*
[3] *Physics and Astronomy Department, UCL, London, WC1E 6BT, UK*
(Dated: February 9, 2008)

Mechanisms for the production of $^1S_0$ diproton pairs, $\{pp\}_s$, in the $pd \to \{pp\}_s n$ reaction are studied at proton beam energies 0.5 – 2 GeV in kinematics similar to those of backward elastic pd scattering. This reaction provides valuable information on the short-range NN and pd interactions that is complementary to that investigated in the well known $pd \to dp$ and $dp \to p(0^\circ)X$ processes. The $pd \to \{pp\}_s n$ reaction is related to the subprocesses $\pi^0 d \to pn$ and $pN \to \{pp\}_s \pi$ using two different one–pion–exchange (OPE) diagrams. Within both these models a reasonable agreement could be obtained with the data below 1 GeV. The similar energy dependence of the $pd \to \{pp\}_s n$ and $pd \to dp$ cross sections and the small ratio of about 1.5% in the production of $\{pp\}_s$ to deuteron final states follow naturally within the OPE models.

PACS numbers: 25.10.+s, 25.40.Qa, 25.45.-z
Keywords: proton–deuteron collisions; diproton production; large momentum transfer reactions

I. INTRODUCTION

There is a long standing problem connected with understanding the mechanism of proton–deuteron backward elastic scattering at energies above 0.5 GeV. This can be formulated as follows. Except in the Δ–isobar region of $0.4 - 0.6$ GeV, the unpolarized differential cross section $\mathrm{d}\sigma/\mathrm{d}\Omega(pd \to dp)_{\theta_{cm}=180^\circ}$ can be explained qualitatively within the impulse approximation (IA) up to large nucleon momenta in the deuteron $k \approx 1$ GeV/c, whereas the experimental values of the tensor analyzing power T_{20} are in strong contradiction to the IA calculations already for $k > 0.3$ GeV/c [1, 2, 3]. Here IA means the one–nucleon–exchange (ONE) mechanism of Fig. 1a which, if it dominated the unpolarized cross section, would allow one to probe directly the high–momentum components in the deuteron wave functions.

A very similar problem arises in the analysis of the inclusive disintegration of the deuteron on nuclear targets, $dA \to p(0^\circ)X$, when the ONE mechanism of Fig. 1b is used to describe the process [4, 5, 6]. In contrast, the tensor polarization t_{20} of the recoil deuteron in elastic electron–deuteron scattering follows very well the IA predictions [7] up to very high transferred momenta $Q = 1.3$ GeV/c, *i.e.* up to $k \sim Q/2 = 0.65$ GeV/c, if realistic phenomenological NN potentials [8, 9, 10] are used to describe the deuteron. Corrections from meson–exchange currents are sizable, but do not change the picture qualitatively [11]. We must conclude that in exclusive and inclusive pd collisions at high transferred momenta we are dealing, not only with the short-range structure of the deuteron, but also with the specific dynamics of the pd interaction and that these dynamics are entirely different from those in the $ed \to ed$ process.

The above contradictions, referred to as the T_{20}-puzzle, can be ascribed, in part, to contributions from the excitation of nucleon isobars (Δ, N^*) in the intermediate state, which were neglected within the IA analysis [1, 2, 3, 4, 5, 6]. For example, the Δ–mechanism seems to dominate the large angle unpolarized $pd \to dp$ cross section in the 0.4–0.6 GeV interval [12, 13, 14]. However, the spin structure of the three–body forces related to the Δ-isobar is far from well established [15]. This therefore leads to ambiguities in any explanation of T_{20} when the Δ–isobar is included in the transition amplitude [12, 13, 14]. It was suggested that, in order to clarify the role of the $\Delta-$isobar, the $pd \to \{pp\}_s n$ reaction should be studied [16, 17, 18]. Due to isospin

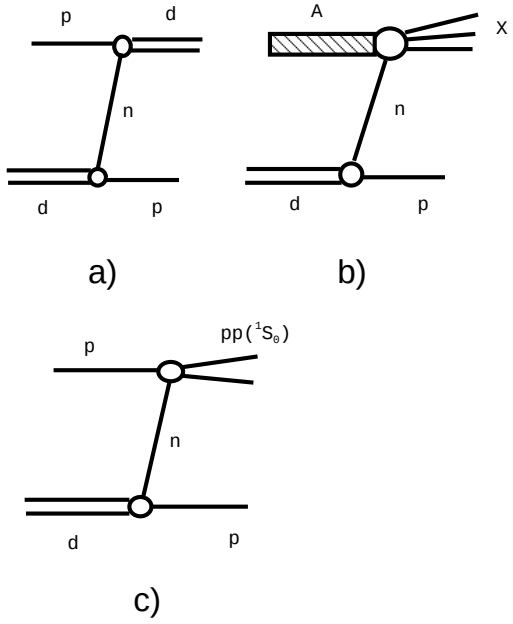

FIG. 1: The one nucleon exchange (ONE) mechanisms of the reactions (a) $pd \to dp$, (b) $dA \to p(0^\circ)X$, and (c) $pd \to \{pp\}_s n$.

invariance, the Δ-mechanism is diminished by a factor of nine in the $pd \to \{pp\}_s n$ cross section as compared to that of $pd - dp$, whereas the ONE mechanism does not suffer a similar suppression [19]. Therefore, the comparison of the two reactions might allow one to get a clearer picture of the relative importance of the ONE and Δ-contributions.

The unpolarized $pd \to \{pp\}_s n$ differential cross section has been measured for large neutron c.m. angles with respect to an incident proton beam which had laboratory kinetic energies in the range $0.6 - 1.9\,\mathrm{GeV}$ [20]. The predominance of the $^1S_0$ state was guaranteed by selecting diproton events with excitation energy $E_{pp} < 3\,\mathrm{MeV}$. An analysis of these data was performed within a model, originally suggested to describe the $pd \to dp$ reaction [12], that included one–nucleon exchange (ONE) (Fig. 1c), single pN scattering, and double scattering with the excitation of the Δ–isobar [21]. This showed that the contribution of the ONE mechanism in Born approximation is actually quite small for a wide range of commonly used NN potentials. Only for a soft NN potential, such as the CD Bonn [10], and with absorptions taken into account in the initial and final states, can a qualitative agreement with data be achieved [21]. In the other extreme, harder NN-potentials, *e.g.* the Paris [22] or especially the Reid soft core [23], generate intense high–momentum components in the NN wave functions and therefore lead to very large ONE contributions that are in strong disagreement with the $pd \to \{pp\}_s n$ data [20]. This is the most interesting observation resulting from the $pd \to \{pp\}_s n$ analysis of Ref. [21].

On the experimental side, the next step towards unraveling the dynamics of the $pd \to \{pp\}_s n$ reaction will be the measurement of the deuteron tensor analyzing power T_{20} [24]. On the theoretical front, an important task is to study other mechanisms that are less sensitive to high NN momentum components than the ONE mechanism. A new and independent analysis of the $pd \to \{pp\}_s n$ dynamics has been made possible through the recent publication of data on the $pp \to \{pp\}_s \pi^0$ reaction [25].

In this paper we analyze the mechanisms of the $pd \to \{pp\}_s n$ reaction that are connected with two–step processes involving the creation and absorption of pions in the intermediate state. The one–pion–exchange (OPE) triangle diagram depicted in Fig. 2a, and here denoted as OPE-I, was initially invoked to describe the large angle $pd \to dp$ reaction [26]. Here the $pd \to dp$ cross section was connected to that for the $pp \to d\pi^+$ sub process at the same beam energy. The predictions of the model were found to be in qualitative agreement with the data on the energy dependence of the pd backward elastic scattering around 0.5–1.0 GeV. An important role of the OPE mechanism, through the $p\{NN\} \to {}^3\mathrm{He}\,\pi$ sub processes, was also found in the reaction $p\,{}^3\mathrm{He} \to {}^3\mathrm{He}p$ at 0.5–1 GeV [27]. To apply the analogous mechanism of Fig. 2b to the $pd \to \{pp\}_s n$ reaction we need to know the amplitudes for both $pp \to \{pp\}_s \pi^0$ and $pn \to \{pp\}_s \pi^-$. At present, however, only the unpolarized cross section for

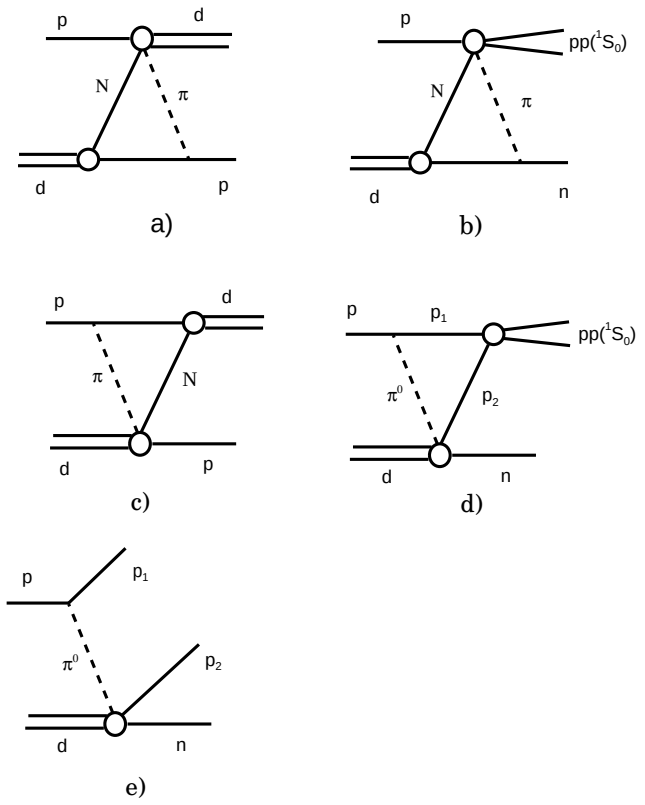

FIG. 2: The one–pion–exchange (OPE) mechanisms considered for the reactions $pd \to dp$ (a,c) and $pd \to \{pp\}_s n$ (b,d,e): OPE-I – a,b; OPE-II – c,d,e.

$pp \to \{pp\}_s \pi^0$ was measured at 0.8 GeV [25]. In the absence of data on π^- production, we have to make assumptions about the $pN \to \{pp\}_s \pi$ mechanism in order to add coherently the contributions from the $pp \to \{pp\}_s \pi^0$ and $pn \to \{pp\}_s \pi^-$ sub processes. The mechanisms used in the present analysis are depicted in Fig. 3. We show in Sec. II that the results of the calculation within OPE-I depend strongly on the mechanism assumed.

Such an ambiguity does not, however, appear for mechanisms with the $\pi^0 d \to pn$ sub process (Fig. 2d and e), which we refer to as OPE-II and discuss in Sec. III. Due to time-reversal invariance, the predictions of OPE-I and OPE-II would be the same for the unpolarized $pd \to dp$ cross section, though this identity does not extend to the analyzing powers. However, to avoid double–counting, one should never consider together the diagrams in Fig. 2a and c, since they may be but different approximations to the same underlying physics. We finally consider in Sec. IV the role of baryon (or Reggeon) exchange in these reactions, that is motivated in part by the results of the recent measurement of the $pp \to \{pp\}_s \pi^0$ reaction [25]. Numerical results for the different models and the comparison with experiment are presented in Sec. V and our conclusions in Sec. VI.

II. THE OPE-I MECHANISM

In the OPE-I approach to the $pd \to \{pp\}_s n$ reaction, the sub process $pN \to \{pp\}_s \pi$ is invoked but, as shown in Fig. 2b, there are contributions with either a π^0 (A^0) or a π^- meson (A^-) in the intermediate state. The coherent sum of these diagrams depends on the contribution of $T = 1/2$ exchange in the pion–production amplitude. Using the mechanisms depicted in Fig. 3, and assuming isospin invariance, we obtain the following results for the deuteron breakup amplitude:

$$A^0(pd \to \{pp\}_s n) + A^-(pd \to \{pp\}_s n) = \begin{cases} 2A^0(pd \to \{pp\}_s n), & \Delta \text{ in } \pi N\text{-rescattering, Fig. 3a} \\ -A^0(pd \to \{pp\}_s n), & N \text{ or } N^* \text{ in } \pi N \text{ rescattering, Fig. 3b} \\ 3A^0(pd \to \{pp\}_s n), & T = \frac{1}{2} \text{ baryon exchange in } t\text{–channel, Fig. 3c} \end{cases} \quad (1)$$

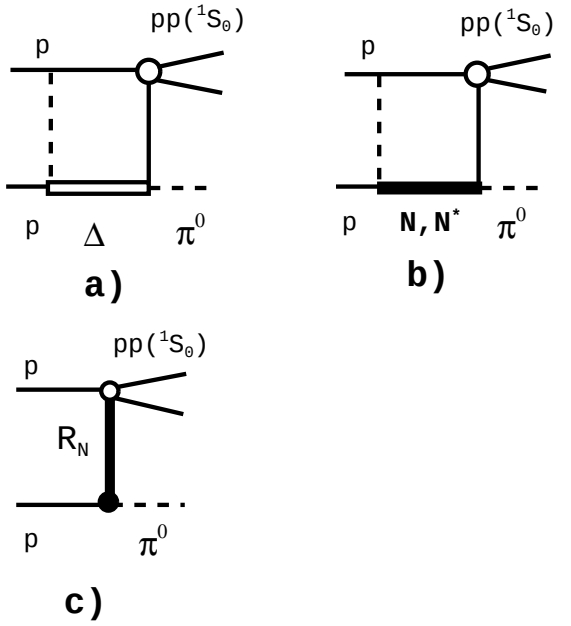

FIG. 3: Possible mechanisms for the $pp \to \{pp\}_s \pi^0$ reaction: (a) Δ-isobar excitation in πN-rescattering, (b) πN- rescattering in the $T = \frac{1}{2}$ state (nucleon or N^* in the s–channel), (c) $T = \frac{1}{2}$ baryon (N, N^*) or Reggeon exchange (BRE) in the t–channel.

The evaluation of the $A(pd \to \{pp\}_s n)$ amplitude of Fig. 2b can be performed using a similar treatment to that of Ref. [28] for the OPE diagram in $pd \to dp$ (Fig. 2a). The resulting c.m. differential cross section has the form

$$\frac{\mathrm{d}\sigma}{\mathrm{d}\Omega}^{OPE-I}(pd \to \{pp\}_s n) = C_j \frac{p_f}{p_i} \frac{q_{pp}}{q_{\pi\{pp\}}} \frac{s_{pp}}{s_{pd}} \frac{f^2_{\pi NN}}{m^2_\pi} \frac{E_n + m}{E^2_n} 4m^2 F^2_\pi(k^2_\pi) \times \Big\{ |Z_0|^2 + |Z_2|^2 \Big\} \frac{\mathrm{d}\sigma}{\mathrm{d}\Omega}(pp \to \{pp\}_s \pi^0), \quad (2)$$

where $f_{\pi NN}$ is the πNN coupling constant, with $f^2_{\pi NN}/4\pi = 0.0796$, m_π and m are the masses of the pion and the nucleon, respectively, k_π is the four–momentum of the virtual pion, $F_{\pi NN}(k^2_\pi) = (\Lambda^2 - m^2_\pi)/(\Lambda^2 - k^2_\pi)$ is the πNN form factor, E_n is the total energy of the final neutron in the laboratory system, p_i and p_f are c.m. momenta in the initial and final states of the reaction $pd \to \{pp\}_s n$, respectively, s_{ij} is the squared invariant mass, and q_{ij} is the relative momentum in the system $j + i$. It is assumed that the cross sections on the left and right hand sides of Eq. (2) are to be taken at the same beam energy and the c.m. production angle of the neutron and π^0 are both equal to 180°. The beam energy for the reaction $pp \to \{pp\}_s \pi$ determines uniquely the values s_{pp}, q_{pp} and $q_{\pi\{pp\}}$.

The coefficient C_j ($j = a, b, c$) depends on the isospin dependence of the $NN \to \{pp\}_s \pi$ reaction. Using Eq. (1) we find for the mechanisms depicted in Fig. 3a, b and c, respectively, $C_a = 1$, $C_b = 4$ and $C_c = 9$. The transition form factors Z_L are defined through

$$Z_0 = \kappa |\mathbf{p}_n| F_0(p_I) - i\Phi_{10}(p_I, \delta_I), \quad (3)$$
$$Z_2 = \kappa |\mathbf{p}_n| F_2(p_I) - \frac{i}{\sqrt{5}} \Big[\sqrt{3}\Phi_{32}(p_I, \delta_I) - \sqrt{2}\Phi_{12}(p_I, \delta_I) \Big],$$

where

$$F_L(p_I) = i^L \int_0^\infty j_L(p_I r) u_L(r) \exp(-\delta_I r)\, r\, \mathrm{d}r,$$
$$\Phi_{lL}(p_I, \delta_I) = i^l \int_0^\infty j_l(p_I r) u_L(r)(1 + \delta_I r) \exp(-\delta_I r)\, \mathrm{d}r, \quad (4)$$

and $u_0(r)$ and $u_2(r)$ are the S– and D–state components of the deuteron wave function, respectively, normalized as

$$4\pi \int_0^\infty [u^2_0(r) + u^2_2(r)]\, r^2 \mathrm{d}r = 1. \quad (5)$$

In Eqs. (4), $j_l(pr)$ is the spherical Bessel function. Kinematical variables are defined as

$$\delta_I^2 = \frac{T_n^2}{(E_n/m)^2} + \frac{m_\pi^2}{E_n/m},$$
$$\kappa = -\frac{m}{E_n}\frac{T_n}{E_n+m}, \mathbf{p}_I = \frac{\mathbf{p}_n}{E_n/m}, \quad (6)$$

where E_n, $\mathbf{p}_n$ and $T_n = E_n - m$ are the total energy, three–momentum, and kinetic energy of the final neutron in the rest frame of the initial deuteron.

For the $pd \to dp$ reaction, the sum of the OPE-I amplitudes with the π^0 and π^+ mesons in the intermediate state is $A^{\pi^0}_{pd\to dp} + A^{\pi^+}_{pd\to dp} = 3A^{\pi^0}_{pd\to dp}$, independent of the model for pion production, as found also in Ref. [29]. Using this result with Eq. (1), and neglecting the difference between the masses of the deuteron and diproton, there is a relation between the c.m. cross sections of the $pd \to \{pp\}_s n$ and $pd \to dp$ reactions within the OPE-I model:

$$\frac{\mathrm{d}\sigma}{\mathrm{d}\Omega}^{OPE-I}(pd \to \{pp\}_s n) = R_I \times \frac{\mathrm{d}\sigma}{\mathrm{d}\Omega}^{OPE-I}(pd \to dp). \quad (7)$$

The factor R_I depends on the mechanism of pion production depicted in Fig. 3 through

$$R_I = \begin{cases} \frac{4}{9}r, \text{ Fig. 3a,} \\ \frac{1}{9}r, \text{ Fig. 3b,} \\ r, \text{ Fig. 3c,} \end{cases} \quad (8)$$

where r is the ratio

$$r = \frac{\mathrm{d}\sigma}{\mathrm{d}\Omega}(pp \to \{pp\}_s\pi^0) \Big/ \frac{\mathrm{d}\sigma}{\mathrm{d}\Omega}(pn \to d\pi^0). \quad (9)$$

The cross sections in Eq. (9) are to be taken at the same beam energy and scattering angle.

III. THE OPE-II MECHANISM

In the OPE-II approach, the deuteron breakup is driven by the $\pi d \to pN$ sub process. The contribution of the diagram of Fig. 2c to pd backward elastic scattering, as well as to the $pd \to \{pp\}_s n$ reaction, were not considered in Refs. [26, 28, 29]. We therefore analyze these amplitudes in somewhat greater detail.

A. The $pd \to \{pp\}_s n$ reaction

For the deuteron breakup reaction $pd \to \{pp\}_s n$, we consider the sum of the two diagrams shown in Fig. 2d and 2e. The $pp\pi^0$ vertex function is

$$A^{\nu_1}_{\nu_p}(p \to \pi^0 p_1) = \frac{f_{\pi NN}}{m_\pi} < \chi_{\nu_1}|\boldsymbol{\sigma}\cdot\mathbf{Q}|\chi_{\nu_p} > \times(\boldsymbol{\tau}\cdot\boldsymbol{\phi}_\pi)2mF_{\pi NN}(k_\pi^2). \quad (1)$$

Here $\boldsymbol{\sigma}$ and $\boldsymbol{\tau}$ are the Pauli matrices for spin and isospin, respectively, χ_{ν_i} is the Pauli spinor with ν_i being the z-projection of the spin of the i'th proton ($i = 1, p$), $\boldsymbol{\phi}_\pi$ is the isospin state of the pion, and $\mathbf{Q}$ is the three–momentum defined as

$$\mathbf{Q} = \sqrt{\frac{E_p+m}{E_{p_1}+m}}\mathbf{p}_1 - \sqrt{\frac{E_{p_1}+m}{E_p+m}}\mathbf{p}_p \approx \sqrt{\frac{E_p+m}{E_{p_1}+m}}(\mathbf{p}_1 - \frac{2m}{E_p+m}\mathbf{p}_p), \quad (2)$$

with $\mathbf{p}_i$ and E_i being the momentum and total energy of the i'th proton. The half–off–shell pp scattering amplitude is (see, for example, Ref. [17])

$$A_{\nu_1\nu_2}(pp \to \{pp\}_s) = N_{pp}\,4m^2 < \psi^{(-)}_{\mathbf{k}}|V(^1S_0)|\mathbf{q} >= -4m^2 N_{pp}(\tfrac{1}{2}\nu_1\tfrac{1}{2}\nu_2|00)4\pi\int_0^\infty j_0(qr)V_s(r)\,\psi^{(-)}_{\mathbf{k}}(\mathbf{r})\,r^2\mathrm{d}r, \quad (3)$$

where ν_1 and ν_2 are the projections of the initial proton spins. In Eq. (3), $\psi^{(-)}_{\mathbf{k}}(\mathbf{r})$ is the pp scattering wave function that is the solution of the Schrödinger equation with the interaction potential $V(^1S_0)$ for a c.m. momentum $|\mathbf{k}|$. It satisfies the following asymptotic boundary condition:

$$\psi^{(-)}_{\mathbf{k}}(\mathbf{r}) \to \frac{\sin(kr+\delta)}{kr}, \quad (4)$$

where δ is the $^1S_0$ phase shift. For simplicity of presentation, we omit here the Coulomb interaction, though this is taken into account in the actual numerical calculations. The combinatorial factor $N_{pp} = 2$ takes into account the identity of the two protons.

The amplitude for the triangle diagram in Fig. 2d is given by the following four–dimensional integral

$$A^{triangle}(pd \to \{pp\}_s n) = \int \frac{\mathrm{d}^3p_1\mathrm{d}T_1}{i(2\pi)^4}\sum_{\nu_1\nu_2}\frac{A^{\nu_1}_{\nu_p}(p\to\pi^0p_1)A^{\nu_2\nu_n}_{\lambda}(\pi^0 d\to pn)A_{\nu_1\nu_2}(pp\to\{pp\}_s)}{(2m)^2(m_\pi^2-k_\pi^2-i\varepsilon)(\mathbf{p}_1^2/2m-T_1-i\varepsilon)(\mathbf{p}_2^2/2m-T_2-i\varepsilon)}, \quad (5)$$

where T_i, $\mathbf{p}_i$, ν_i are the kinetic energy, three–momentum and projection of the spin of the intermediate i'th proton

$(i = 1, 2)$, respectively. Closing the contour of integration in the lower–half T_1 plane, and taking into account the residue at the point $T_1 = \mathbf{p}_1^2/2m - i\varepsilon$, one finds from Eq. (5) that

$$A^{triangle}(pd \to \{pp\}_s n) = -N_{pp} \sum_{\nu_1 \nu_2} (\tfrac{1}{2}\nu_1 \tfrac{1}{2}\nu_2|00) \times \int \frac{\mathrm{d}^3 p_1}{(2\pi)^3} \frac{A_\lambda^{\nu_2 \nu_n}(\pi^0 d \to pn) < \psi_{\mathbf{k}}^{(-)}|V(^1S_0)|\mathbf{q} > m}{(m_\pi^2 - k_\pi^2 - i\varepsilon)(\mathbf{q}^2 - \mathbf{k}^2 - i\varepsilon)} \times A_{\nu_p}^{\nu_1}(p \to \pi^0 p_1). \quad (6)$$

The pole diagram with an intermediate π^0 meson depicted in Fig. 2e leads to the following amplitude

$$A^{pole}(pd \to \{pp\}_s n) = \frac{A_{\nu_p}^{\nu_{p1}}(p \to \pi^0 p_1) A_\lambda^{\nu_{p2} \nu_n}(\pi^0 d \to pn)}{m_\pi^2 - k_\pi^2 - i\varepsilon}, \quad (7)$$

where ν_{p_1} and ν_{p_2} are the projections of the spins of the two final protons that are in the $^1S_0$ state. There is another pole diagram with an intermediate π^+ meson but this can be safely neglected here because it does not lead to low energy pp pairs.

Making the coherent sum of the triangle and the properly antisymmetrized pole amplitudes, given respectively by Eq. (6) and Eq. (7), we find

$$A_{\nu_p \lambda}^{\nu_n}(pd \to \{pp\}_s n) = A^{triangle} + A^{pole} = N_{pp} \frac{f_{\pi NN}}{m_\pi} 2m F_{\pi NN}(k_\pi^2) \sum_{\nu_1 \nu_2} (\tfrac{1}{2}\nu_1 \tfrac{1}{2}\nu_2|00) A_\lambda^{\nu_{p_2} \nu_n}(\pi^0 d \to pn) \int \frac{\mathrm{d}^3 p_1}{(2\pi)^3} \frac{< \chi_{\nu_1}|(\boldsymbol{\sigma} \cdot \mathbf{Q})|\chi_{\nu_p} > \Psi_{\mathbf{k}}^{(-)^*}(\mathbf{q})}{m_\pi^2 - k_\pi^2 - i\varepsilon}\,. \quad (8)$$

We have here used the Lippmann–Schwinger equation

$$\psi_{\mathbf{k}}^{(-)^*}(\mathbf{q}) = (2\pi)^3 \delta^{(3)}(\mathbf{q} - \mathbf{k}) - \frac{m < \psi_{\mathbf{k}}^{(-)}|V(^1S_0)|\mathbf{q} >}{\mathbf{q}^2 - \mathbf{k}^2 - i\varepsilon}\,. \quad (9)$$

The integral over $\mathbf{p}_1$ in Eq. (8) can be evaluated in the rest frame of the final diproton, where $\mathbf{p}_1 = \mathbf{q}$, as was done for the $pd \to dp$ reaction [28]. With this in mind, the kinematic variables $\mathbf{Q}$ and the pion propagator are rewritten as:

$$\begin{aligned} \mathbf{Q} &= \sqrt{\frac{E_p + m}{2m}} \{(\mathbf{p}_1 - \mathbf{p}_{II}) + \mathbf{R}\}, \\ \mathbf{p}_{II} &= \frac{\mathbf{p}_p}{E_p/m}, \quad \mathbf{R} = -\frac{m}{E_p} \frac{T_p}{E_p + m} \mathbf{p}_p, \\ k^2 - m_\pi^2 &= -\frac{E_p}{m} \left\{(\mathbf{p}_1 - \mathbf{p}_{II})^2 + \delta_{II}^2\right\}, \\ \delta_{II}^2 &= \frac{T_p^2}{(E_p/m)^2} + \frac{m_\pi^2}{E_p/m}, \end{aligned} \quad (10)$$

where E_p, $\mathbf{p}_p$ and $T_p = E_p - m$ are the total energy, three–momentum and kinetic energy of the initial proton in the rest frame of the final diproton.

Values of the $pd \to \{pp\}_s n$ cross section were presented in Ref. [20] with a cut–off in the pp excitation energy of $E_{pp}^{max} = 3\,\mathrm{MeV}$. Defining the corresponding maximum relative momentum through $k_{max} = \sqrt{m\, E_{pp}^{max}}$, the c.m. differential cross section becomes [17]

$$\frac{\mathrm{d}\sigma}{\mathrm{d}\Omega_n}(pd \to \{pp\}_s n) = \frac{1}{(4\pi)^5} \frac{p_f}{p_i} \int_0^{k_{max}} \mathrm{d}k \frac{k^2}{s_{pd}\sqrt{m^2 + \mathbf{k}^2}} \times \frac{1}{2} \int \mathrm{d}\Omega_{\mathbf{k}}\, \overline{|A(pd \to \{pp\}_s n)|^2}. \quad (11)$$

The factor of 1/2 in front of the angular integration in Eq. (11) takes into account the identity of two final protons.

We choose the reference frame where the final diproton is at rest and let the quantization axis OZ lie along the direction of the initial proton $\mathbf{p}_p$. In this frame only the longitudinal components ($\mu = 0$) of the vectors $\mathbf{p}_{II}$ and $\mathbf{R}$ are non–zero. Thus the spin–averaged–squared amplitude of the $pd \to \{pp\}_s n$ reaction can be written in the following factorized form:

$$\overline{|A^{triangle} + A^{pole}|^2} = \frac{1}{4} |N_{pp} \frac{f_{\pi NN}}{m_\pi} 2m\, F_{\pi NN}(k_\pi^2)|^2 \times \Big| \int \frac{\mathrm{d}^3 q}{(2\pi)^3} \frac{Q^{\mu=0}}{k_\pi^2 - m_\pi^2 + i\varepsilon}\, \psi_k^{(-)^*}(\mathbf{q}) \Big|^2 \overline{|A(\pi^0 d \to pn)|^2}, \quad (12)$$

where $\overline{|A(\pi^0 d \to pn)|^2}$ is the spin–averaged–squared amplitude of the $\pi^0 d \to pn$ reaction. This factorization is a consequence of the simple spin structure of the diproton vertex $pp \to \{pp\}_s$.

For the $^1S_0$ final state, $\overline{|A(pd \to \{pp\}_s n)|^2}$ does not depend upon the direction of the proton momentum $\mathbf{k}$ in the diproton rest frame, so that the integration over $\mathrm{d}\Omega_{\mathbf{k}}$ merely gives a 4π factor. The cross section can be finally written as:

$$\frac{\mathrm{d}\sigma}{\mathrm{d}\Omega_n}^{OPE-II}(pd \to \{pp\}_s n) = \frac{1}{3\pi^2} \frac{p_f}{p_i} \frac{q_{pn}}{q_{\pi d}} \frac{s_{pn}}{s_{pd}} \Big[\frac{f_{\pi NN}}{m_\pi} 2m F_{\pi NN}(k_\pi^2)\Big]^2 \frac{\mathrm{d}\sigma}{\mathrm{d}\Omega}(pn \to d\pi^0) \times \int_0^{k_{max}} \mathrm{d}k \frac{k^2}{\sqrt{m^2 + k^2}} |J_{pp}^{\mu=0}(p_{II}, \delta_{II})|^2. \quad (13)$$

The form factor $\mathbf{J}_{pp}$ is defined through

$$\mathbf{J}_{pp}(p_{II},\delta_{II}) = \int \frac{\mathrm{d}^3q}{(2\pi)^3}\frac{\mathbf{Q}}{k_\pi^2 - m_\pi^2 + i\varepsilon}\,\psi_k^{(-)^*}(\mathbf{q}) = \sqrt{\frac{E_p+m}{2m}}\frac{m}{E_p}\left\{\mathbf{R}F_0(p_{II},\delta_{II}) - i\hat{\mathbf{p}}_p\,\Phi_k^{pp}(p_{II},\delta_{II})\right\}, \tag{14}$$

$$F_0 = \int_0^\infty \mathrm{d}r\, r\, j_0(p_{II}\, r)\exp\left(-\delta_{II} r\right)\psi_{\mathbf{k}}^{(-)^*}(\mathbf{r}), \tag{15}$$

$$\Phi_k^{pp} = i\int_0^\infty \mathrm{d}r(\delta_{II} r + 1) j_1(p_{II} r)\exp\{-\delta_{II} r\}\,\psi_{\mathbf{k}}^{(-)^*}(\mathbf{r}), \tag{16}$$

where the kinematic variables $\mathbf{R}$, $\mathbf{p}_{II}$, δ_{II} are determined by Eq. (10).

B. The $pd \to dp$ reaction

The OPE-II diagram for the reaction $pd \to dp$, depicted in Fig. 2c, includes two contributions corresponding to a π^+ (A^+) and a π^0 (A^0) in the intermediate state. Using isospin invariance, the coherent sum of these diagrams is equivalent to that with π^0 multiplied by an isospin factor of 3: $A^+ + A^0 = 3A^0$.

For the $pn \to d$ vertex one has

$$A_{\nu_p\nu_n}^{\lambda'}(pn \to d) = -4m\sqrt{m}\left(\varepsilon + \frac{\mathbf{q}^2}{m}\right)\varphi_{\lambda'}^{\nu_p\nu_n\,^*}(\mathbf{q}), \tag{17}$$

where $\varphi_{\lambda'}^{\nu_p\nu_n}(\mathbf{q})$ is the deuteron wave function in momentum space

$$\varphi_{\lambda'}^{\nu_p\nu_n}(\mathbf{q}) = \sum_{L,M_L,M_S}(\tfrac{1}{2}\nu_p\tfrac{1}{2}\nu_n|1M_S) \times(LM_L1M_S|1\lambda)\,Y_{LM_L}(\hat{\mathbf{q}})\,u_L(q), \tag{18}$$

with Clebsch–Gordan coefficients and spherical harmonics in standard notation and $u_0(q)$ and $u_2(q)$ being respectively the S– and D–state components. The wave function is normalized as

$$\frac{1}{3}\sum_{\nu_p\,\nu_n\,\lambda}\int\frac{\mathrm{d}^3q}{(2\pi)^3}|\varphi_\lambda^{\nu_p\nu_n}(\mathbf{q})|^2 = \int_0^\infty\Big[u_0^2(q) + u_2^2(q)\Big]q^2\frac{\mathrm{d}q}{(2\pi)^3} = 1. \tag{19}$$

The total $pd \to dp$ transition amplitude becomes

$$A_{\nu_p\lambda}^{\nu_p'\lambda'}(pd \to dp) = 3\frac{f_{\pi NN}}{m_\pi}F_{\pi NN}(k_\pi^2)2\sqrt{m} \times\sum_{\nu_1,\nu_2,\mu}\sqrt{3}(1\mu\tfrac{1}{2}\nu_p|\tfrac{1}{2}\nu_1)\int\frac{\mathrm{d}^3q}{(2\pi)^3}\frac{\tilde{Q}^\mu}{k^2 - m_\pi^2 + i\varepsilon} \times\varphi_{\lambda'}^{\nu_1\nu_2}(\mathbf{q})A_\lambda^{\nu_2\nu_p'}(\pi^0 d \to pn), \tag{20}$$

where ν_p (ν_p') andλ (λ') are the spin projections of the initial (final) proton and deuteron.

The integral over the three–momentum $\mathbf{q}$ of the intermediate nucleon is evaluated in the rest frame of the final deuteron. There it takes the form

$$J_L^\mu(\tilde{p},\delta) = \int\frac{\mathrm{d}^3q}{(2\pi)^3}\frac{\tilde{Q}^\mu\,\varphi_\lambda^{\nu_1\nu_2}(\mathbf{q})}{k^2 - m_\pi^2 + i\varepsilon} = \sqrt{\frac{E_p+m}{2m}}\frac{m}{E_p}\left\{R^\mu F_L(\tilde{p},\delta) - i\hat{\mathbf{p}}_p^\mu\Phi_{1L}(\tilde{p},\tilde{\delta})\right\}, \tag{21}$$

where the quantization axis is chosen to lie along $\mathbf{p}_p$. The kinematical variables $\tilde{\mathbf{Q}}$, $\tilde{p}$ and $\tilde{\delta}$ come from Eqs. (10) for the variables $\mathbf{Q}$, p_{II} and δ_{II}, with E_p, $\mathbf{p}_p$ and T_p being replaced respectively by the total energy $\tilde{E}_p = \sqrt{m^2 + \tilde{\mathbf{p}}_p^2}$, three–momentum $\tilde{\mathbf{p}}_p$, and kinetic energy $\tilde{T}_p = \tilde{E}_p - m$ of the initial proton in the rest frame of the final deuteron. The form factors F_L and Φ_{lL} are defined by Eqs. (4).

Finally, the c.m. $pd \to dp$ differential cross section is predicted to be:

$$\frac{\mathrm{d}\sigma}{\mathrm{d}\Omega}^{OPE-II}(pd \to dp) = 9\Big[\frac{f_{\pi NN}}{m_\pi}2\sqrt{m}F_{\pi NN}(k_\pi^2)\Big]^2\frac{s_{pn}}{s_{pd}} \times\frac{q_{pn}}{q_{\pi d}}\Big\{|J_0^{\mu=0}(\tilde{p},\tilde{\delta})|^2 + |J_2^{\mu=0}(\tilde{p},\tilde{\delta})|^2\Big\}\frac{\mathrm{d}\sigma}{\mathrm{d}\Omega}(pn \to d\pi^0). \tag{22}$$

For backward proton–deuteron elastic scattering, the $pp \to d\pi^+$ cross section is also to be taken for a similar forward–going deuteron. Since Eq. (22) coincides with Eq. (1) of Ref. [29], the OPE-II and OPE-I models give the same formula for the unpolarized $pd \to dp$ cross section, as required.

On the basis of Eqs. (13) and (22), we can find the following factor relating the $pd \to \{pp\}_s n$ and $pd \to dp$ differential cross sections to be compared to that in Eq. (7):

$$R_{II} = \frac{m}{27\pi^2}\int_0^{k_{max}}\mathrm{d}k\frac{k^2}{\sqrt{m^2 + k^2}}|\Phi_k^{pp}(p_{II},\delta_{II})|^2\Big/\,|\Phi_{10}^d(\tilde{p},\tilde{\delta})|^2, \tag{23}$$

where the integrals $\Phi_{10}^d(\tilde{p},\tilde{\delta})$ and $\Phi_k^{pp}(p_{II},\delta_{II})$ are determined by Eqs. (4) and (16), respectively. Approximating the integral in Eq. (23) by using the value of the integrand at $\overline{E}_{pp} = E_{pp}^{max}/2$, one can rewrite the equation as

$$R_{II} \approx \frac{2}{27}\frac{k_{max}^3}{6\pi^2 m}\frac{|\Phi_{\overline{k}}^{pp}(p_{II},\delta_{II})|^2}{|\Phi_{10}^d(\tilde{p},\tilde{\delta})|^2}, \tag{24}$$

where $\overline{k} = \sqrt{2\,m\,\overline{E}_{pp}}$. In the derivation of R_{II} we have neglected the contribution of the deuteron D–state component and the form factor F_L, which are, however, included in the numerical evaluations.

The origins of the different terms in Eq. (24) are easy to understand. To obtain Eq. (22) from (13) one needs to make the following replacements: (i) $\psi_{\mathbf{k}}^{(-)}(\mathbf{r}) \to \varphi_d(\mathbf{r})/\sqrt{m}$; (ii) multiply by the ratio of the isospin and combinatorial factors $9/\left(N_{pp}^2/2\right) = 9/2$; (iii) multiply by the spin factor of three; (iv) multiply by the factor $4\pi^2$, which arises from the difference between three– and two–body phase spaces; (v) divide by the factor

$$\int_0^{k_{max}} \frac{k^2}{\sqrt{m^2+k^2}} \mathrm{d}k \approx \frac{k_{max}^3}{3m}. \qquad (25)$$

IV. THE EXCHANGE OF BARYONS WITH $\mathbf{T = \frac{1}{2}}$ IN THE t–CHANNEL

The baryon exchange (BE) amplitude for $pd \to \{pp\}_s n$ of Fig. 4c can be written as:

$$A^{BE}(pd \to \{pp\}_s n) = \sum_{\nu_N} \frac{A_\lambda^{\nu_N \nu_n}(d \to pN^*) A_{\nu_p \nu_N}(pN^* \to \{pp\}_s)}{m_{N^*}^2 - t - i\varepsilon}, \qquad (1)$$

where m_{N^*} is the mass of the exchanged baryon, ν_N its spin projection, $t = (p_d - p_n)^2$ the four–momentum transfer, and $A_{\nu_p \nu_N}(pN^* \to \{pp\}_s)$ and $A_\lambda^{\nu_N \nu_n}(d \to pN^*)$ the amplitudes of the sub processes $pN^* \to \{pp\}_s$ and the vertex $d \to pN^*$ respectively. While the case of one–nucleon–exchange can be found in Refs. [17, 18, 21], the formalism for N^* with higher spins was studied in Ref. [30], where a good fit to the cross section data on the $pd \to dp$ and $pp \to d\pi^+$ reactions was obtained for beam energies $T_p > 1\,\mathrm{GeV}$.

For our present purposes, the main features of the BE mechanism are (i) its isospin structure with $T = \frac{1}{2}$ in the t–channel, and (ii) the factorized residue of the amplitude. The same features are present in the Reggeon mechanism, where the transition amplitude is given by

$$A(s,t) = F(t)\Big(\frac{s}{s_0}\Big)^{\alpha_N(t)} \exp\Big[-i\frac{\pi}{2}\left(\alpha_N(t) - \tfrac{1}{2}\right)\Big], \qquad (2)$$

where $\alpha_N(t)$ is the nucleon Regge trajectory. The residues of the Regge amplitudes $F(t)$ can be factorized into products of terms coming from the upper and lower vertices of Fig. 4. Therefore, within the baryon or Reggeon exchange (BRE) model, one obtains the following relation between the c.m. cross sections:

$$\frac{\mathrm{d}\sigma}{\mathrm{d}\Omega}^{BRE}(pd \to \{pp\}_s n) = \frac{\frac{\mathrm{d}\sigma}{\mathrm{d}\Omega}(pp \to \{pp\}_s \pi^0)}{\frac{\mathrm{d}\sigma}{\mathrm{d}\Omega}(pn \to d\pi^0)} \times \frac{\mathrm{d}\sigma}{\mathrm{d}\Omega}^{BRE}(pd \to dp). \qquad (3)$$

Here the cross sections, within the BRE model of Fig. 4, are taken at the same four–momentum transfer t for all reactions and at $s = s_{pp} \approx s_{pn}$ for the $pn \to d\pi^0$ and $pp \to \{pp\}_s \pi^0$, and $s = s_{pd}$ for the $pd \to \{pp\}_s n$ and $pd \to dp$ reactions. In deriving this relation we assume that the t-dependence of the vertices is smooth. Formally Eq. (3) coincides with Eq. (7) with $R_I = 1$.

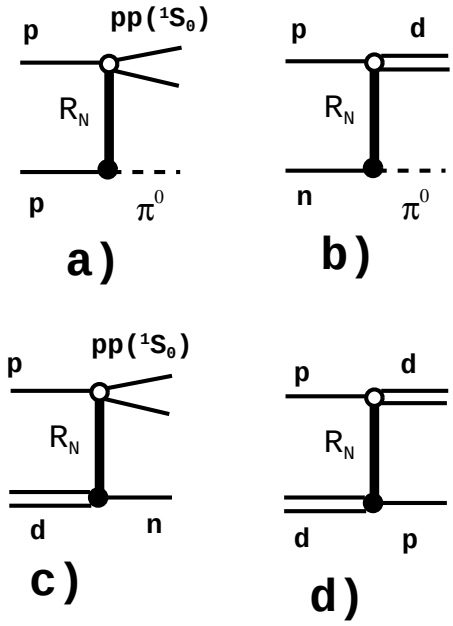

FIG. 4: The exchange of baryons with isospin $T = \frac{1}{2}$ (N, N*, and Reggeon) in the t–channel of the $pp \to \{pp\}_s\pi^0$, $pn \to d\pi^0$, $pd \to \{pp\}_s n$ and $pd \to dp$ reactions.

V. RESULTS AND DISCUSSION

A. The OPE-II model

The results of our calculations are shown in Figs. 5 and 6. For the $pd \to dp$ differential cross section, the OPE-I and OPE-II approaches give identical results and they reproduce the observed shoulder in the energy dependence in the $T_p = 0.5 - 0.7\,\mathrm{GeV}$ region, which is caused by virtual Δ excitation [12, 13, 14, 21, 26]. At higher energies, $T_p > 1\,\mathrm{GeV}$, the OPE cross section falls faster than the data. The calculated cross sections varies very weakly with increasing cut-off parameter Λ in the πNN vertex.

The OPE-II model for $pd \to \{pp\}_s n$ is in reasonable agreement with the experimental data below 1 GeV, being best at about 0.8 GeV. It is interesting to note that at this energy and $\theta_{cm} = 180°$ the ONE mechanism vanishes due to a repulsive core in the NN-interaction, as illustrated in Fig. 6 [21]. As a result, double scattering with the excitation of the $\Delta(1232)$-isobar was found to be dominant in this region. Since $pn \to d\pi^0$ is also Δ–dominated in this region, the agreement between the OPE-II model and the $pd \to \{pp\}_s n$ data seems largely to confirm the results of Ref. [21]. Furthermore, at this kinematic point the ONE amplitude changes sign, as does the ONE–OPE interference.

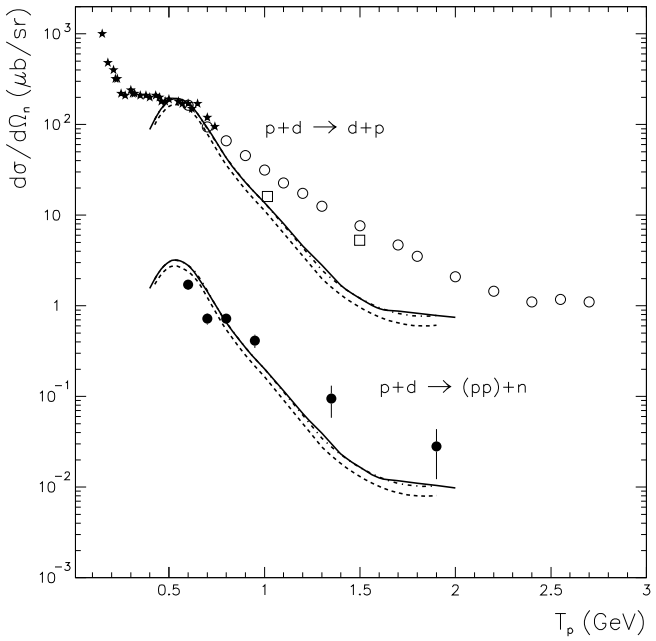

FIG. 5: The differential cross sections for $pd \to dp$ at $\theta_{c.m.} = 180^o$ and $pd \to \{pp\}_s n$ averaged over $\theta_{c.m.} = 166^\circ - 180^\circ$ *versus* the proton beam energy compared with the predictions of the OPE-II model for different values of the cut-off parameter: $\Lambda = 1\,\mathrm{GeV/c}$ (full line), 0.8 (dashed-dotted), 0.65 GeV/c (dashed). The cross section of the $pn \to d\pi^0$ reaction is taken from the SAID SP96 solution [31]. Data for $pd \to \{pp\}_s n$ and $pd \to dp$ are those of Ref. [20] and [32, 33, 34] respectively.

Outside this region, the ONE mechanism gives a sizable contribution [18, 21], which suggests that the disagreement between the data and the OPE-II model away from $T_p \approx 0.8\,\mathrm{GeV}$ may be connected with the ONE contribution. In Fig. 6 we show the ONE (DWBA) contribution taken from Ref. [21] and its coherent sum with the OPE contribution, with the relative sign being chosen to get the best agreement with the data [20]. We are here implicitly assuming that ONE is negligible in the physical $\pi^0 d \to pn$ amplitude.

Above 1 GeV, the cross section for the $pd \to \{pp\}_s n$ reaction calculated in the OPE-II model falls faster than the data with increasing energy. In this model the energy slope for both this and the $pd \to dp$ reaction is determined mainly by the energy dependence of the cross section of the $pn \to d\pi^0$ reaction; other kinematic factors and form factors are very smooth functions of the beam energy. As a result, the ratio of diproton to deuteron formation is practically independent of T_p.

As explained in Sec. III B, the strong preference for deuteron formation within the OPE-II mechanism is the result of several considerations, including spin–isospin, combinatorial, phase space factors as well as the ratio of form factors in Eq. (23). For a maximum diproton excitation energy of $E_{pp}^{max} = 3\,\mathrm{MeV}$ and beam energy in the interval $0.6 - 1.9\,\mathrm{GeV}$, Eqs. (23, 24) predict a ratio of $R_{II} \approx 0.016 - 0.013$, which is in qualitative agreement with the experimental value $R^{exp} = 0.010 - 0.011$ [20].

In contrast to the OPE-II model, within the OPE-I formalism of Eq. (8) the small magnitude of the ratio R_I follows mainly from the small ratio of the cross sections of the $pp \to \{pp\}_s \pi^0$ and $pn \to d\pi^0$ reactions, as seen from Ref. [25] at 0.8 GeV. Results within this approach will remain ambiguous until there is more information on the $pn \to \{pp\}_s \pi^-$ amplitude.

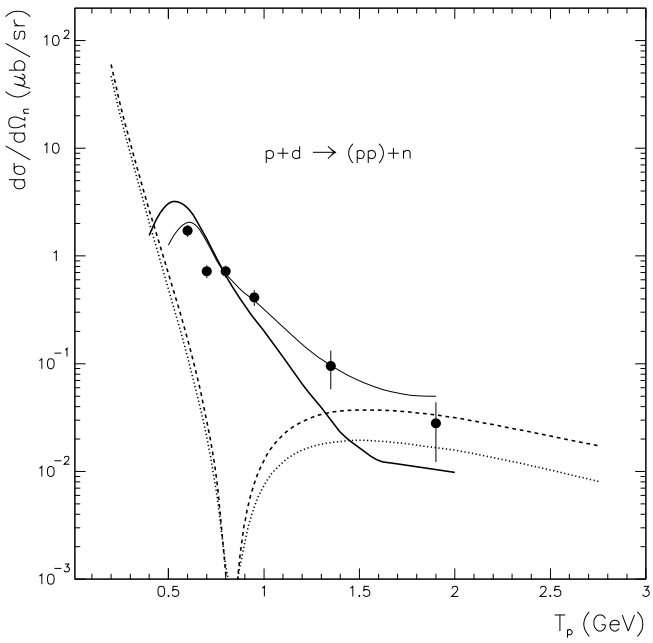

FIG. 6: Differential cross section for the $pd \to \{pp\}_s n$ reaction [20]. The full thick curve shows the OPE-II results for $\Lambda = 1\,\mathrm{GeV/c}$. The predictions [21] of the ONE(DWBA) mechanism with the CD Bonn potential are shown by the dashed (Born approximation) and dotted (with distortions) curves. The coherent sum of the OPE-II and the ONE(DWBA) is shown by the thin full line.

B. The OPE-I and BRE models

At present the OPE-I approach can only be compared with the $pd \to \{pp\}_s n$ data at 0.8 GeV, where results on the $pp \to \{pp\}_s \pi^0$ have recently appeared [25]. Assuming that the BRE mechanism of Fig. 3c dominates the $pN \to \{pp\}_s \pi$ amplitude at this energy, we find from Eq. (7) a value of the $pd \to \{pp\}_s n$ differential cross section of $0.7\mu\mathrm{b}/sr$, which is in a good agreement with the data [20]. On the other hand, if the $\Delta-$isobar mechanism dominates pion production at 0.8 GeV [35], then the OPE-I approach falls too low by a factor two. Graphs

with an intermediate N^*, as in Fig. 3b, would make the underestimate a factor of nine.

If the BRE mechanism is indeed important for the $pp \to \{pp\}_s\pi^0$ reaction at 0.8 GeV, one should analyze the role of this mechanism also in the $pn \to d\pi^0$, $pd \to \{pp\}_s n$ and $pd \to dp$ reactions. Using the $pp \to \{pp\}_s\pi^0$ data [25] and the SAID SP96 solution [31] for the $pn \to d\pi^0$ reaction, we find from Eq. (3) that the BRE model also predicts the same value of 0.7 μb/sr for the $pd \to \{pp\}_s n$ cross section. Within the Reggeon model, the small magnitude of the $pd \to \{pp\}_s n$ cross section, as compared to the $pd \to dp$, should be considered to be consequence of the relative sizes of the residue functions at the $pR_N\{pp\}$ and $pR_N d$ vertices.

In order to get more insight into the dynamics of the $pd \to \{pp\}_s n$ and $pp \to \{pp\}_s\pi^0$ reactions one has to discriminate between the BRE and the Δ-isobar mechanism of the reaction $pp \to \{pp\}_s\pi^0$ at 0.8 GeV (and higher energies). For this purpose it is important to measure the unpolarized cross section of the $pn \to \{pp\}_s\pi^-$ reaction since

$$\frac{\mathrm{d}\sigma}{\mathrm{d}\Omega}(\pi^0)/\frac{\mathrm{d}\sigma}{\mathrm{d}\Omega}(\pi^-) = \begin{cases} 2, & \Delta-\text{mechanism}, \\ \frac{1}{2}, & T = \frac{1}{2}\ t\text{–channel exchange}. \end{cases} \tag{1}$$

C. The Reggeon mechanism and constituent–quark counting rules

We have shown that the OPE-II model can explain the similarity in the energy dependence of the $pd \to dp$ and $pd \to \{pp\}_s n$ cross sections but underestimates both of their overall values at $T_p = 1 - 2$ GeV. It was argued that this discrepancy might be due to contributions from ONE or baryon (Reggeon) exchanges. If this is true, it would mean that the effective degrees of freedom in these reactions are non–nucleonic. In this connection it is interesting to check whether the constituent-quark counting rules (CCR) [36, 37] can be applied to these reactions. A scaling behavior related to the CCR was observed in the $\gamma d \to pn$ reaction at photon beam energy 1–4 GeV (see Refs. [38, 39] and references therein). Recently the CCR behavior was found also in the $pd \to dp$ and $dd \to {}^3\mathrm{H}p$ reactions in the GeV energy region at large scattering angles [40]. This suggests that one might usefully search for a similar CCR behavior in the $pd \to dp$ and $pd \to \{pp\}_s n$ reactions, at least in the region between the $\Delta(1232)$ and $\Delta(1920)$ resonances, say between 1 and 2 GeV.

According to the CCR hypothesis, the energy dependence of the invariant cross sections can be parameterized as

$$\frac{\mathrm{d}\sigma}{\mathrm{d}t} = \frac{\pi}{p_i p_f}\frac{\mathrm{d}\sigma}{\mathrm{d}\Omega_{cm}} = \frac{1}{s^n} f(\theta_{cm}), \tag{2}$$

where the function $f(\theta_{cm})$ does not depend on energy and $n+2$ is the sum of all active point-like constituents in the initial and final states. Our fit to the data shown in Fig. 7 gives $n = 12.9$ for both the $pd \to \{pp\}_s n$ and $pd \to dp$ reactions, whereas CCR would suggest that $n = 3+6+3+6-2 = 16$. One would therefore require significant diquark configurations in order to get better numerical agreement.

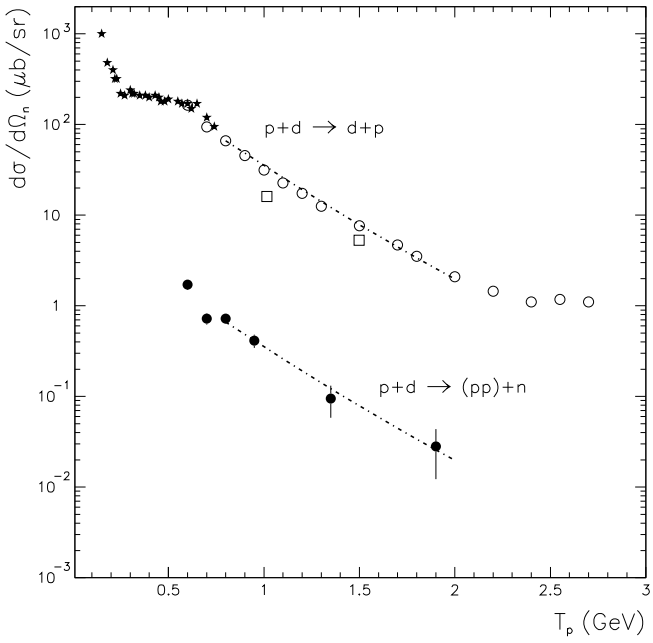

FIG. 7: Differential cross sections for the $pd \to dp$ and $pd \to \{pp\}_s n$ reactions as shown in Fig. 5. The dashed–dotted lines give the results of fitting the data within the CCR approach of Eq. (2), where the invariant cross section behaves as $\frac{\mathrm{d}\sigma}{\mathrm{d}t} = const \times s^{-12.9}$.

VI. CONCLUSIONS

The present analysis shows that there are close connections between the different reactions which lead to diproton formation in the final state in pd and pN-collisions. However, the actual relations depend on the reactions mechanisms. We found that the predictions of the OPE-II model, which is based on the $\pi^0 d \to pn$ sub process, are quite close to the $pp \to \{pp\}_s n$ deuteron breakup data. This model allows us to explain the absolute value of the $pd \to \{pp\}_s n$ cross section at $\theta_{cm} \approx 180°$ in the Δ–isobar region 0.6 – 0.9 GeV as well as its energy dependence. It also describes the small value of the ratio $R = \mathrm{d}\sigma(pd \to \{pp\}_s n)/\mathrm{d}\sigma(pd \to dp)$ in the whole interval 0.6 – 1.9 GeV of measurement reported in Ref. [20].

The agreement points to an important contribution coming from the $\Delta-$isobar below 1 GeV, which enters *via* the $\pi^0 d \to pn$ sub process but, on the other hand, suggests that the ONE mechanism is relatively unimportant. To a large extent, these conclusions are compatible

with the results of the previous analysis of this reaction, performed on the basis of a different model [21]. The minor role found for the ONE contribution sheds some light on the T_{20} puzzle, discussed in the introduction, which is entirely based on the assumption that the ONE mechanism dominates the large momentum–transfer pd reactions.

There is as yet insufficient information to describe the $pd \to \{pp\}_s n$ data unambiguously within the OPE-I model. However, if we assume the dominance of $T = \frac{1}{2}$ exchange in the $pN \to \{pp\}_s \pi$ amplitude, as given for example by baryon or Reggeon exchange, then a satisfactory description can be achieved. Much of this ambiguity will be removed once data are available from the forthcoming measurements of the cross sections for $pp \to \{pp\}_s \pi^0$ and $pp \to \{pp\}_s \pi^-$ at $\theta_{cm} \approx 0^\circ$ in the 1 – 2 GeV region [41].

Acknowledgments

The authors are grateful to J. Niskanen for useful discussions. Two of the authors (YuU and CW) wish to recognize the hospitality of the Institut für Kernphysik of the Forschungszentrum Jülich, where much of this work was carried out. This work was supported in part by the Heisenberg–Landau programme.

[1] J. Arvieux *et al.*, Phys. Rev. Lett. **50**, 19 (1983); Nucl.Phys. A **431**, 613 (1984).
[2] V. Punjabi *et al.*, Phys. Lett. B **350**, 178 (1995).
[3] L.S. Azhgirey *et al.*, Phys. Lett. B **391**, 22 (1997); Yad. Fiz. **61**, 494 (1998).
[4] C.F. Perdrisat, *et al.*, Phys. Rev. Lett. **59**, 2840 (1987).
[5] V.G. Ableev *et al.*, Pis'ma Zh. Eksp. Teor. Fiz. **47**, 558 (1988).
[6] L.S. Azhgirey *et al.*, Phys. Lett. B **387**, 37 (1996).
[7] R. Gilman and F. Gross, J. Phys. G **28**, R37 (2002).
[8] V.G.J. Stoks, R.A.M. Klompt, C.P.F. Terheggen, and J.J. de Swart, Phys. Rev. C **49**, 2950 (1994).
[9] R.B. Wiringa, V.G.J. Stoks, and R. Schiavilla, Phys. Rev. C **51**, 38 (1995).
[10] R. Machleidt, Phys. Rev. C **63**, 024001 (2000).
[11] H. Arenhövel, F. Ritz, and T. Wilbois, Phys. Rev. C **61**, 034002 (2000).
[12] L.A. Kondratyuk, F.M. Lev, and L.V. Schevchenko, Yad. Fiz. **33**, 1208 (1982).
[13] A. Boudard and M. Dillig, Phys. Rev. C **31**, 302 (1985).
[14] Yu.N. Uzikov, Phys. Part. Nucl. **29**, 583 (1998).
[15] H. Sakai *et al.*, Phys. Rev. Lett. **84**, 5288 (2000).
[16] O. Imambekov and Yu.N. Uzikov, Yad. Fiz. **52**, 1362 (1990) (Sov. J. Nucl. Phys. **52**, 862 (1990)).
[17] A.V. Smirnov and Yu.N. Uzikov, Phys. At. Nucl. **61**, 361 (1998).
[18] Yu.N. Uzikov, J. Phys. G **28**, B13 (2002).
[19] Yu.N. Uzikov, Pis'ma Zh. Eksp. Theor. Fiz. **75**, 7 (2002).
[20] V.I. Komarov *et al.*, Phys. Lett. B **553**, 179 (2003).
[21] J. Haidenbauer and Yu.N. Uzikov, Phys. Lett. B **562**, 227 (2003).
[22] M. Lacombe *et al.*, Phys. Rev. C **21**, 861 (1980).
[23] J.R.V. Reid, Ann. Phys. **50**, 411 (1968).
[24] A. Kacharava, F. Rathmann, and C. Wilkin, *Spin Physics at COSY*, arXiv:nucl-ex:0511028.
[25] S. Dymov *et al.*, Phys. Lett. B **635**, 270 (2006).
[26] N.S. Craigie and C. Wilkin, Nucl. Phys. **B14**, 477 (1969).
[27] Yu.N. Uzikov and J. Haidenbauer, Phys. Rev. C **68**, 014001 (2003).
[28] V.M. Kolybasov and N.Ya. Smorodynskaya, Yad. Fiz. **17**, 1211 (1973).
[29] L. Vegh, J. Phys. G **5**, L121 (1979).
[30] J.S. Sharma and A.N. Mitra, Phys. Rev. **9** (1974) 2574.
[31] R.A. Arndt, I.I. Strakovsky, R.L. Workman, and D.V. Bugg, Phys. Rev. C **48**, 1926 (1993); http://gwdac.phys.gwu.edu.
[32] L. Dubal *et al.*, Phys. Rev. D **9**, 597 (1974).
[33] A. Boudard, thesis, CEA-N-2386, Saclay (1984).
[34] P. Berthet *et al.*, J. Phys. **G8**, L111 (1982).
[35] J. Niskanen, Phys. Lett. B **642**, 34 (2006).
[36] V.A. Matveev, R.M. Muradyan, and A.N. Tavkhelidze, Nuovo Cim. Lett. **7**, 719 (1973).
[37] S.J. Brodsky and G.R. Farrar, Phys. Rev. Lett. **31**, 1153 (1973).
[38] P. Rossi, M. Mirazita, F. Ronchetti *et al.*, Phys. Rev. Lett. **94**, 012301 (2005).
[39] V.Yu. Grishina, L.A. Kondratyuk, W. Cassing et al, Eur. Phys. J. **A19**, 117 (2004).
[40] Yu.N. Uzikov, Pis'ma Zh. Eksp. Theor. Fiz. **81**, 387 (2005).
[41] A.V. Kulikov, *Measurement of the cross section and analyzing power of the* $\vec{p}p \to \{pp\}_s\pi^0$ *reaction*, COSY proposal No. 158 (2005).